FINAL REPORT

to the

Air Force Office of Scientific Research

TWO- AND THREE- DIMENSIONAL MEASUREMENTS IN TURBULENT NONPREMIXED FLAMES

AFOSR Grant No. F49620-97-1-0096

February 16, 1997 - February 15, 2000

Principal Investigator: Marshall B. Long

Yale University

Department of Mechanical Engineering and Center for Laser Diagnostics

New Haven, Connecticut 06520-8284

May 14, 2000

CONTENTS

	Page
Introduction	1
Research Accomplishments	1
Three-Scalar/Mixture Fraction Imaging	1
OH Fluorescence	3
Sodium Fluorescence	4
Nitrogen Raman	5
Optical Flow Velocimetry	13
Additional Research Developments	17
References	18
Publications Resulting from the Research	20
Scientific Collaborators	21
Degrees Awarded	21
Lectures Presented about the Research	22

INTRODUCTION

Laser diagnostic techniques have been developed at Yale University that are capable of two–dimensional mapping of multiple scalars and velocities in turbulent flames. The techniques are designed to measure quantities and flow configurations of current interest to combustion modelers. The availability of quantitative data on the spatial and temporal characteristics of structures in turbulent reacting flows will aid in understanding the interaction of chemical reactions with the turbulent motion. A better understanding of this key interaction is important for testing existing models of turbulent combustion as well as for suggesting new models.

During the three years of AFOSR support, significant progress has been made in refining the mixture fraction imaging technique and in two critical, related research areas: (1) Three-scalar measurements in turbulent flames, and (2) Optical flow velocimetry techniques based on unseeded scalar image pairs. In the following sections, the major accomplishments are outlined.

RESEARCH ACCOMPLISHMENTS

Three-Scalar/Mixture Fraction Imaging

During the current funding period, significant advances have been made in the refinement of mixture fraction imaging techniques in turbulent nonpremixed flames. The mixture fraction (ξ) is defined as the mass fraction of atoms originating in the fuel stream and is independent of the chemical reaction occurring in the flame. The gradient of the mixture fraction is needed to find the scalar dissipation, which determines the rate of molecular mixing in the flow. The mixture fraction and its gradient are important parameters in the modeling of turbulent flames, and the experimental determination of mixture fraction over a wide field is essential for testing these models.

One method for constructing a conserved scalar suitable for imaging experiments in reacting flows has been through the simultaneous measurement of temperature (T) and fuel concentration [1,2]. The conserved scalar β, is defined based on fuel mass fraction (Y_F) and enthalpy and takes the form:

$$\beta = Y_F + c_p \mathrm{T}/Q \tag{1}$$

where Q is the lower heat of combustion and c_p is the specific heat at constant pressure. This can be cast into an expression for mixture fraction:

$$\xi^{FT} \equiv \frac{\beta - \beta_{air}}{\beta_{fuel} - \beta_{air}} = \frac{Y_F + \left(c_p \mathrm{T} - c_{p,air}\mathrm{T}_{air}\right)/Q}{Y_{F,fuel} + \left(c_{p,fuel}\mathrm{T}_{fuel} - c_{p,air}\mathrm{T}_{air}\right)/Q} \tag{2}$$

This two-scalar approach, which assumes unity Lewis number and idealized one-step reaction between fuel and oxidizer, relates to the measured signals through:

$$\xi^{FT} = \frac{C_1 \sigma}{W\,Ra} Rm + \frac{C_2}{Q}\left(c_p \frac{\sigma}{Ra} - c_{p,air} T_{air} \right) \tag{3}$$

where *Rm* is the measured fuel Raman scattering and *Ra* is the Rayleigh scattering. The parameter σ, which is proportional to the Rayleigh cross section, the mixture molecular weight *W*, and the specific heat c_p, are dependent on the mixture fraction. Strained counterflow flame calculations provide appropriate functional forms for these parameters which are incorporated into an iterative scheme for determining ξ. The remaining constants C_1 and C_2 must be determined from calibration experiments.

In the mixture fraction imaging experiments, the fuel concentration has been obtained using Raman scattering from the fuel. The use of Raman scattering to determine the fuel concentration allows the use of chemically simple fuels such as methane and hydrogen, which are reasonably consistent with the one-step chemistry assumptions implicit in the technique. Earlier experiments using fluorescence from more complex hydrocarbons provided good signal/noise, but suffered inaccuracies in the derived mixture fraction due to loss of parent fuel [3,4].

In a previous funding period, experiments were performed in a variety of nonpremixed flame configurations, including a lifted methane diffusion flame [5]. Data sets were also obtained for piloted methane/air flames [6] and an unpiloted hydrogen flame [7]. In the methane/air flames, the methane was diluted with air (70% by volume) to eliminate soot, and resulted in a stoichiometric mixture fraction of $\xi = 0.29$. The premixed annular pilot flame was a stoichiometric mixture of acetylene, hydrogen, and air, which insured a steadily burning main flame without significant local extinction. The fuel jet issued from a nozzle of diameter 6.1 mm into a filtered, vertical, coflowing 7.0 m/s air stream.

One major issue resolved within this funding period concerns uncertainty in the position of the stoichiometric contour using the two-scalar approach with air-diluted methane flames. While dilution prevents difficulties arising from excessive luminosity (or laser-induced incandescence), it also creates a broader minimum for the Rayleigh scattered signal in mixture fraction space as shown in Fig. 1. Close to the stoichiometric value of the mixture fraction, the fuel concentration approaches zero and the Rayleigh signal remains nearly constant. It was proposed that a suitable third scalar quantity would clarify the accuracy of the two-scalar approach. This could be achieved either by modifying the two-scalar approach or providing simultaneous independent determination of mixture fraction. A detailed study of candidate third scalars led to the in-depth examination of three particular scenarios: (1) OH fluorescence, (2) seeded sodium atomic fluorescence, and (3) nitrogen Raman with a customized fuel mixture.

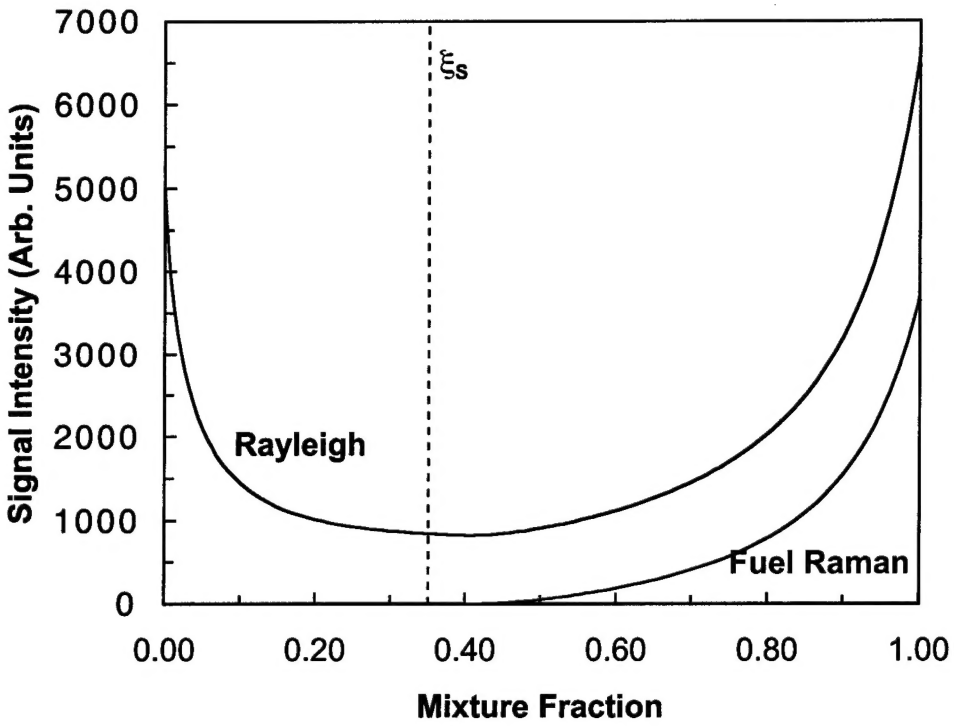

Figure 1. Profiles of signal intensities: Rayleigh scattering and methane Raman scattering scattering as a function of mixture fraction for an air–diluted (3:1 by volume) methane counterflow flame. The signals are scaled to appear on the same plot.

OH Fluorescence Imaging

The first case employed laser-induced fluorescence of the OH radical as an approximate marker of the reaction zone near stoichiometric. Experiments were performed in a *Re*=15,000 turbulent nonpremixed methane flame. The dye laser output was frequency doubled and tuned to excite the $Q_1(7)$ transition of OH (~289 nm) and fluorescence was observed at a wavelength near 309 nm. Laser energy in the ultraviolet was about 2 mJ per pulse. Simultaneous Rayleigh/Raman/OH LIF images taken 25 jet diameters downstream are shown in Fig. 2. The imaged region is 20.5 mm × 4.4 mm, which includes the jet centerline on the left side of the image and a region of ambient air on the other side of the image.

In general, the OH fluorescence does not fill regions where the Rayleigh signal is at a minimum and Raman signal disappears. While this technique offers insight into the local flame structure, it fails to provide a clear advantage in terms of supplementing mixture fraction information that can be calculated from the Rayleigh and Raman signals.

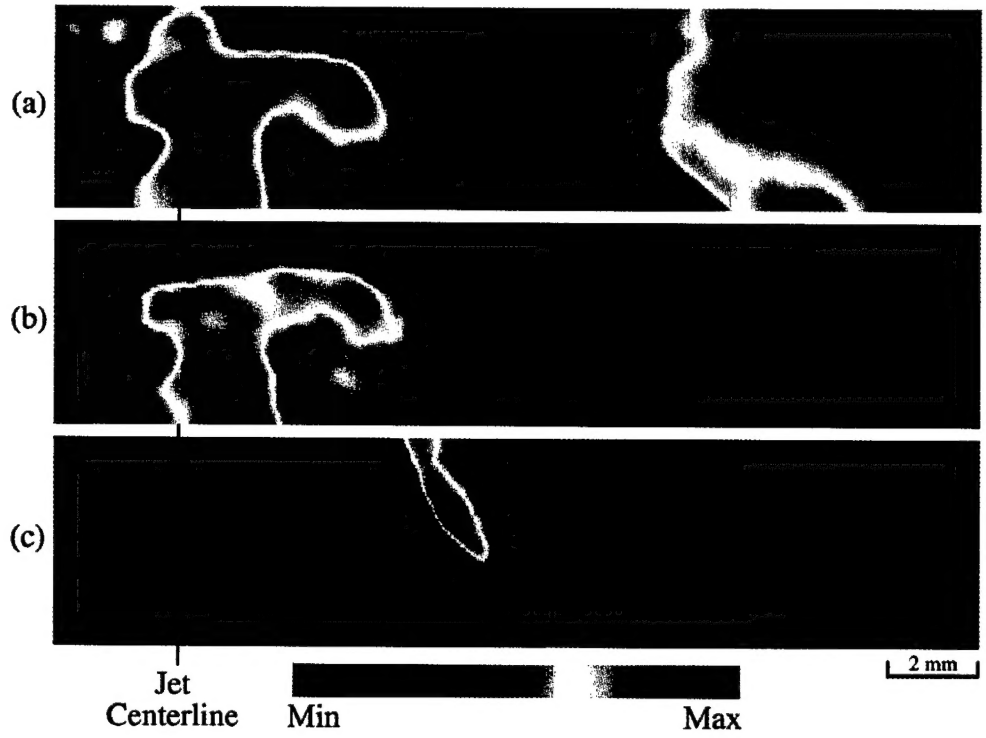

Figure 2. (a) Rayleigh, (b) Raman, and (c) OH fluorescence images from a turbulent nonpremixed methane flame (*Re*=15000) taken 25 jet diameters downstream.

Sodium Fluorescence Imaging

In the past, sodium has been added to flames for applications such as temperature measurements (by the line-reversal technique) and control of soot formation. Laser-induced fluorescence of sodium is well documented [8] although the present work represents the first attempt to assess its applicability as a marker of mixture fraction through the flame zone. Sodium is introduced into the flow using an atomizer (TSI Model 9306) containing a 3.4×10^{-3} M solution of NaCl in initially de-ionized water. The NaCl molecules dissociate due to high temperatures encountered in the flame zone. The Nd:YAG-pumped dye laser is tuned to the $3^2S_{1/2,}\rightarrow3^2P_{1/2,}$ transition of sodium at 589 nm, with output beam energies around 15 mJ. The resulting image represents fluorescence of the $3^2P_{1/2,3/2}$ sodium doublet to the ground state at wavelengths of 589 nm and 589.6 nm, respectively.

Measurements were again made in a turbulent flame (*Re*=15,000) 25 jet diameters downstream as shown in Fig. 3. To a greater extent than with OH LIF, the sodium fluorescence signal fills the region between the Raman and Rayleigh signal, and extends into the fuel region. The peak of the fluorescence occurs in the high temperature region, probably near the stoichiometric contour given the results of laminar flame validation studies. However, Mie scattering from residual salt particles interferes significantly with

the fuel Rayleigh signal prohibiting quantitative determination of mixture fraction. This interference also prevents contour smoothing the Raman image.

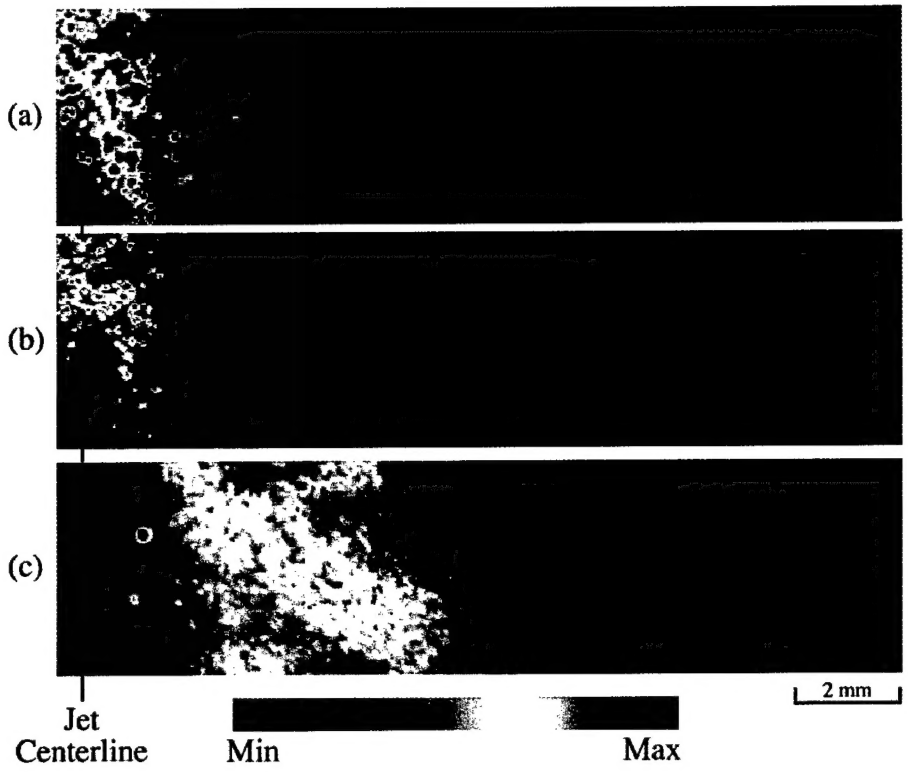

Figure 3. a) Rayleigh, (b) Raman, and (c) sodium fluorescence images from a turbulent nonpremixed methane flame (*Re*=15000) taken 25 jet diameters downstream.

Nitrogen Raman Imaging

The ideal third scalar is a monotonic function of mixture fraction, a trait not exhibited by either OH or sodium. An inert species would have this property if it was present only in either the fuel or oxidizer stream. This concept led to a comprehensive study of imaging nitrogen mass fraction as a third scalar measurement using Raman scattering with a customized fuel mixture [9]. Experiments were performed in which the fuel stream contained no nitrogen, which gave the nitrogen signal the desired characteristic as shown in Fig. 4.

Assuming no significant nitrogen consumption occurs during reaction, we can write the conserved scalar in terms of nitrogen mass fraction:

$$\beta^{N_2} \equiv Y_{N_2} \tag{4}$$

with the mixture fraction:

$$\xi^{N_2} = 1 - \frac{Y_{N_2}}{Y_{N_2,\text{air}}} = 1 - \frac{C_3\,\sigma}{W\,Ra} Rm_{N_2} \tag{5}$$

where Rm_{N_2} is the nitrogen Raman signal, and C_3 is a calibration constant. This formulation requires measurement of the temperature and nitrogen concentration, and thus, represents an additional two-scalar approach.

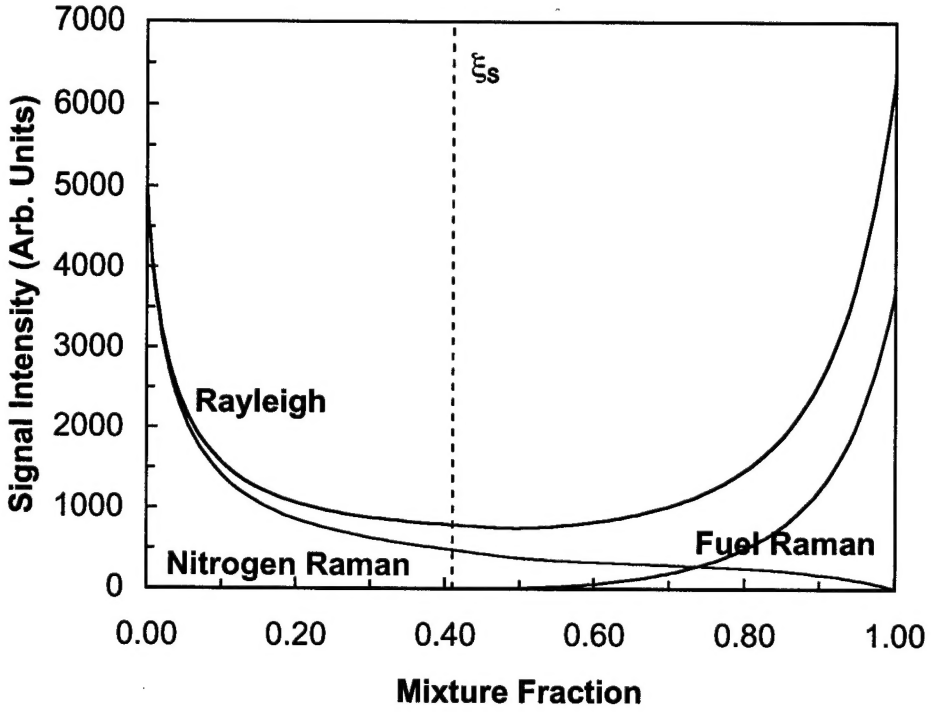

Figure 4. Profiles of signal intensities: Rayleigh scattering, methane Raman scattering, and nitrogen Raman scattering as a function of mixture fraction for an argon/oxygen–diluted methane counterflow flame. The signals are scaled to appear on the same plot.

The customized fuel used in the experiments consists of methane mixed with argon and oxygen to provide an overall 3/1 dilution ratio by volume (3 parts diluent to 1 part fuel). The oxygen content was selected to simulate air dilution, which gives a composition of 25% methane, 59% argon, and 16% oxygen by volume. This fuel mixture has a stoichiometric mixture fraction ξ_s=0.41, putting the reaction zone well inside the shear layer. Counterflow flame calculations (strain rate=100 s^{-1}) of this system

demonstrate the departure of the ξ^{FT} two-scalar formulation from the "actual" mixture fraction (Fig. 5) calculated using the following formula [10]:

$$\xi \equiv \frac{2Z_C/W_C + \frac{1}{2}Z_H/W_H + \left(Z_{O,air} - Z_O\right)/W_O}{2Z_{C,fuel}/W_C + \frac{1}{2}Z_{H,fuel}/W_H + \left(Z_{O,air} - Z_{O,fuel}\right)/W_O} \tag{6}$$

It is predicted from these calculations that the mixture fraction based upon nitrogen mass fraction should exhibit little deviation from the actual ξ. Deviation from one-step chemistry (i.e. loss of parent fuel to intermediate species) is compensated in calculating fuel concentration by the expression $Rm_F = Rm_{F,0}\,(1 + C_F\,\Phi^2)$, where $Rm_{F,0}$ is the uncompensated value, and the reactivity is defined as $\Phi = (T - T_{ambient})/(T_{ad} - T_{ambient})$ [6]. C_F is a weighting coefficient ($C_F = 0.8$) and, as illustrated in the figure by the curve marked ξ_{cor}^{FT}, corrects on the rich side of stoichiometric.

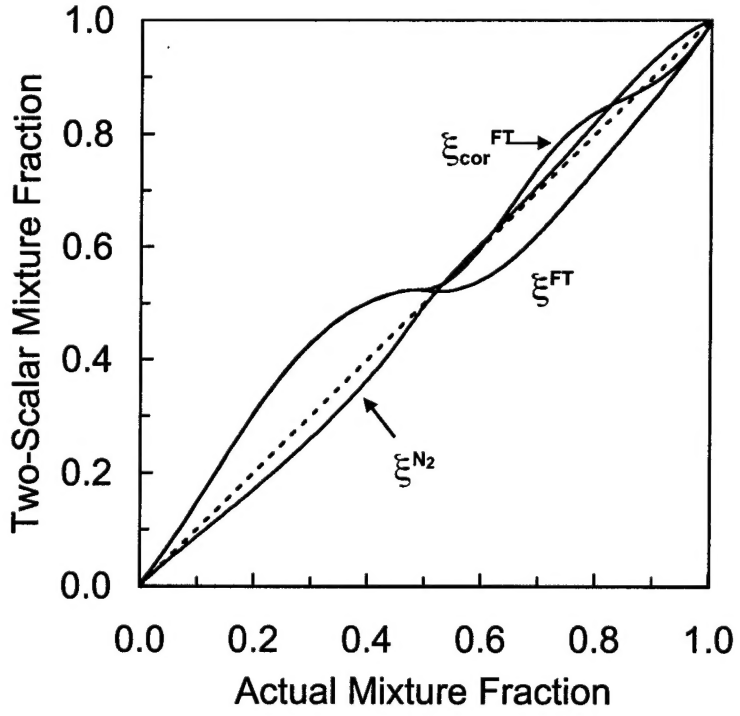

Figure 5. Mixture fraction calculated from strained laminar flame calculations ($100s^{-1}$) using the fuel-temperature (black line) and nitrogen-temperature (blue line) two-scalar approaches plotted against mixture fraction calculated using Equation 3. The effect of fuel correction on ξ^{FT} is also shown (red line).

Simultaneous planar Rayleigh, fuel Raman, and nitrogen Raman images have been collected in experiments using three cameras and a single laser. Figure 6 shows the experimental facility. A flashlamp-pumped dye laser is employed in an intracavity

configuration to generate single-shot energies up to 4.7 J at 532 nm. The beam is focused into a sheet over a 6.1 mm diameter piloted burner. Scattered light is collected on both sides of the flame by low *f*/# camera lenses oriented perpendicular to the laser sheet. The Rayleigh scattering and fuel Raman scattering are collected along the same optical path and divided with a 50/50 pellicle beam splitter, while the weaker nitrogen Raman scattering is collected along the opposite optical path. Image intensifiers are lens-coupled to liquid-cooled CCD cameras and isolated with appropriate interference filters.

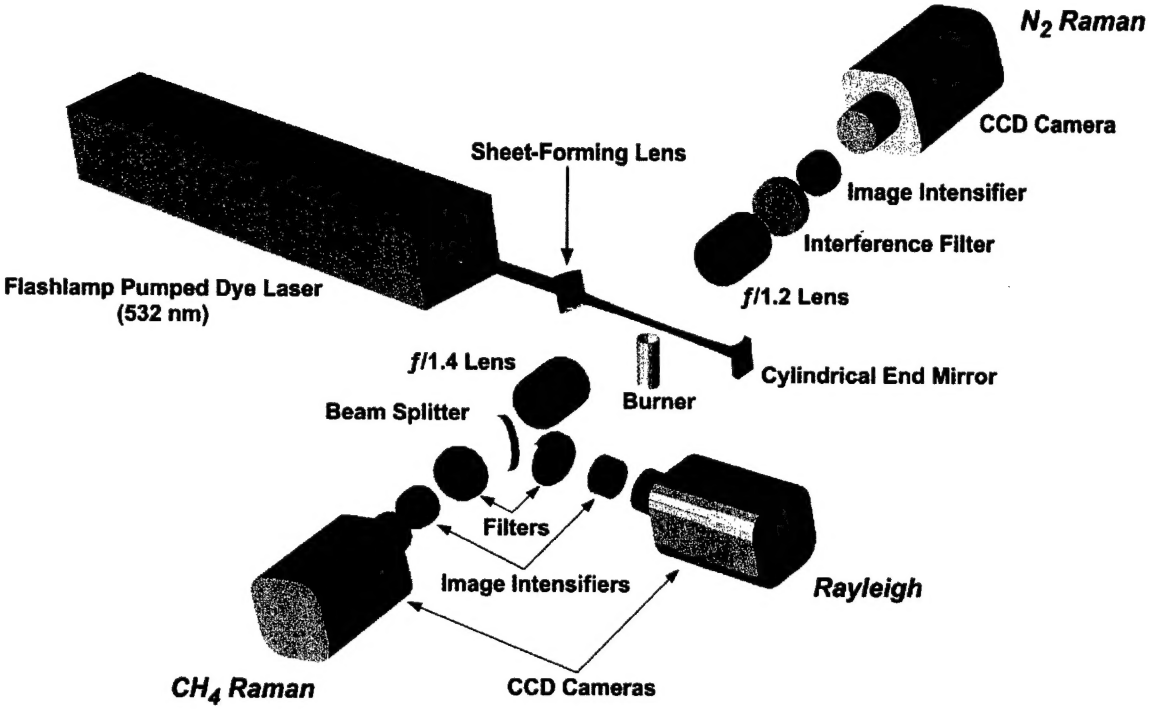

Figure 6. Schematic of the three-scalar turbulent flame imaging experiment.

In the past, the imaging resolution of the optical setup has been characterized in terms of the volume associated with each pixel. For the present work, the pixel volume is 49 × 49 × 500 μm^3, where the largest value corresponds to the laser sheet thickness, and the remaining dimensions describe the area imaged onto a single pixel. The actual spatial resolution is a more complex function of the optical layout, including alignment, lenses, filters, image intensifiers, and camera pixel size. In order to better quantify the spatial resolution for this configuration, simultaneous images have been taken of a uniformly illuminated 25 μm wire located at the focal plane. Individual camera resolutions are based upon the resulting full-width half-maximum (FWHM) intensity of the wire image

from each camera following scaling, translation, rotation, and cropping. The spatial resolution is 170 μm on the Rayleigh camera, 140 μm on the nitrogen Raman camera, and 275 μm on the fuel Raman camera. Translating the wire normal to the plane of the laser sheet within the beam thickness (± 250 μm from the focal plane) has minimal effect (<10%) on the individual camera resolutions.

Because this is a multi-camera experiment and the cameras are located along different optical trains, there remains the issue of how well the images correlate on a pixel-by-pixel basis. Cross-camera spatial resolutions here are defined based upon adding combinations of matched images from each camera, and measuring the resultant full-width half-maximum of the wire. With optimal matching, the on-axis spatial resolution is 280 μm, about equal to the largest single camera resolution. Factors such as distortion may cause degradation away from the optical axis to a maximum measured 400 μm. Using the $1/e^2$ intensity point rather than the FWHM for determining spatial resolution increases the reported values by ~75%.

Estimates of the Kolmogorov scale (κ) on the centerline for a diluted methane flame (3/1 air/methane by volume) give a value of κ=95 μm at *Re*=20,600 [4]. Using this as an approximate value for the turbulent flame in this work, the resolutions reported here are in the range 2-4κ. A study of an isothermal jet performed by Namazian, et al. reports that a spatial resolution of 5κ should be sufficient for capturing 60% of the scalar dissipation spectrum [11]. In flames, where heat release is expected to increase length scales, a resolution of 5κ should be sufficient to record most of the scalar dissipation.

Figure 7 shows line plots of mixture fraction from a laminar flame (Re=1600) at a location 15 nozzle diameters downstream (*D*=6.1 mm). Two curves are shown for ξ^{FT}, which differ in the parameterization of the mixture fraction dependent terms appearing in Eqn. 3 (i.e. σ, W, c_p). The curve marked "No lean correction" uses flame calculation terms parameterized by "actual" mixture fraction determined from the Bilger formula (Equation 6).

To correct ξ^{FT} on the lean side, $c_p(\xi)$, $\sigma(\xi)$, and $W(\xi)$ are described as functions of the *predicted* two-scalar mixture fraction ξ^{FT}, rather than the actual mixture fraction from the flame calculations. Figure 5 showed that the old approach results in a departure of ξ^{FT} from the more rigorous formulation, as indicated by strained laminar flame calculations (100 s^{-1} strain rate). Deviation from one-step chemistry (i.e. loss of parent fuel to intermediate species) is compensated in the curve marked ξ^{FT}_{cor} by using a weighting term involving reactivity. The curve for ξ^{N_2} exhibits little deviation from the actual mixture fraction. By assigning functional dependences based on the predicted ξ^{FT} from flame calculations, the ξ^{FT} curve shown in Fig. 7 is obtained showing improved agreement with ξ^{N_2}. The flame computations are insensitive to variations in the strain rate over the range 10-200 s^{-1}, which is expected to be representative of the scalar dissipation values measured in the turbulent flame, based on existing data in similar flames [6,12].

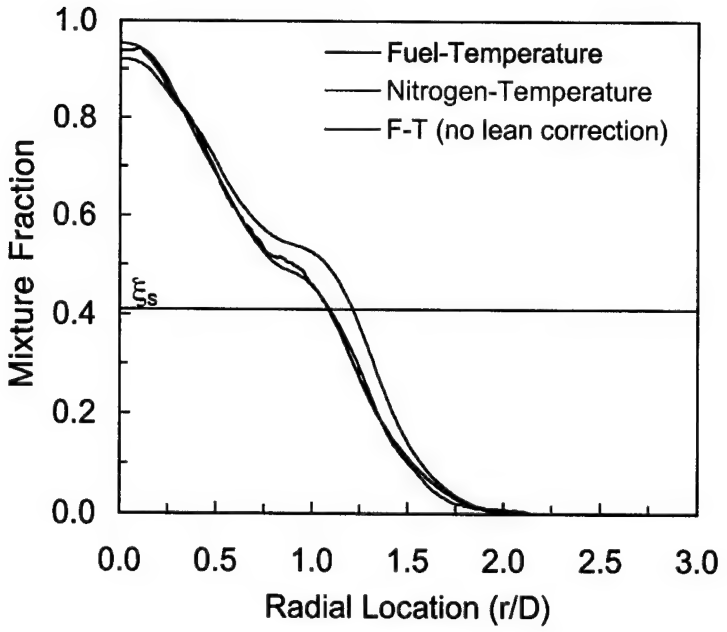

Figure 7. Radial variation of mixture fraction from the modified fuel-temperature (black line) and nitrogen-temperature (blue line) two-scalar approaches in a laminar flame. The unmodified ξ^{FT} approach overpredicts mixture fraction in regions around stoichiometric (red line).

Applying this technique to single-pulse imaging in turbulent nonpremixed flames provides similar results, although the N_2 Raman signal is more affected by noise, especially in regions of high mixture fraction where there is little nitrogen. Figures 8 and 9 show images taken 25*D* downstream from a *Re*=15,000 turbulent flame; the Raman images have been contour smoothed [13]. Qualitatively, the scalar dissipation fields, χ (defined as $\chi \equiv 2\mathcal{D}\,\nabla\xi\cdot\nabla\xi$, where $\mathcal{D}$ is the diffusivity), appear similar, revealing the same main structural features, with significant scalar dissipation apparent along the edge of the main jet. The position of the stoichiometric mixture fraction contour is highlighted (white lines) in Fig. 9.

The experiments measuring nitrogen-temperature mixture fraction have served as a guide for correcting the fuel-temperature mixture fraction for values around and lean of stoichiometric. It has been shown that parameterizing specific heat, molecular weight, and Rayleigh cross section as a function of ξ^{FT} predicted from counterflow flame calculations, rather than the actual mixture fraction, improves the performance of this two-scalar approach. Under turbulent conditions (*Re*=15,000), the two approaches reveal differences close to the centerline, most likely a result of noise limitations of the nitrogen Raman signal. This work increases confidence in employing ξ^{FT} for mixture fraction determination, which remains the most attractive approach because of its superior signal-to-noise characteristics.

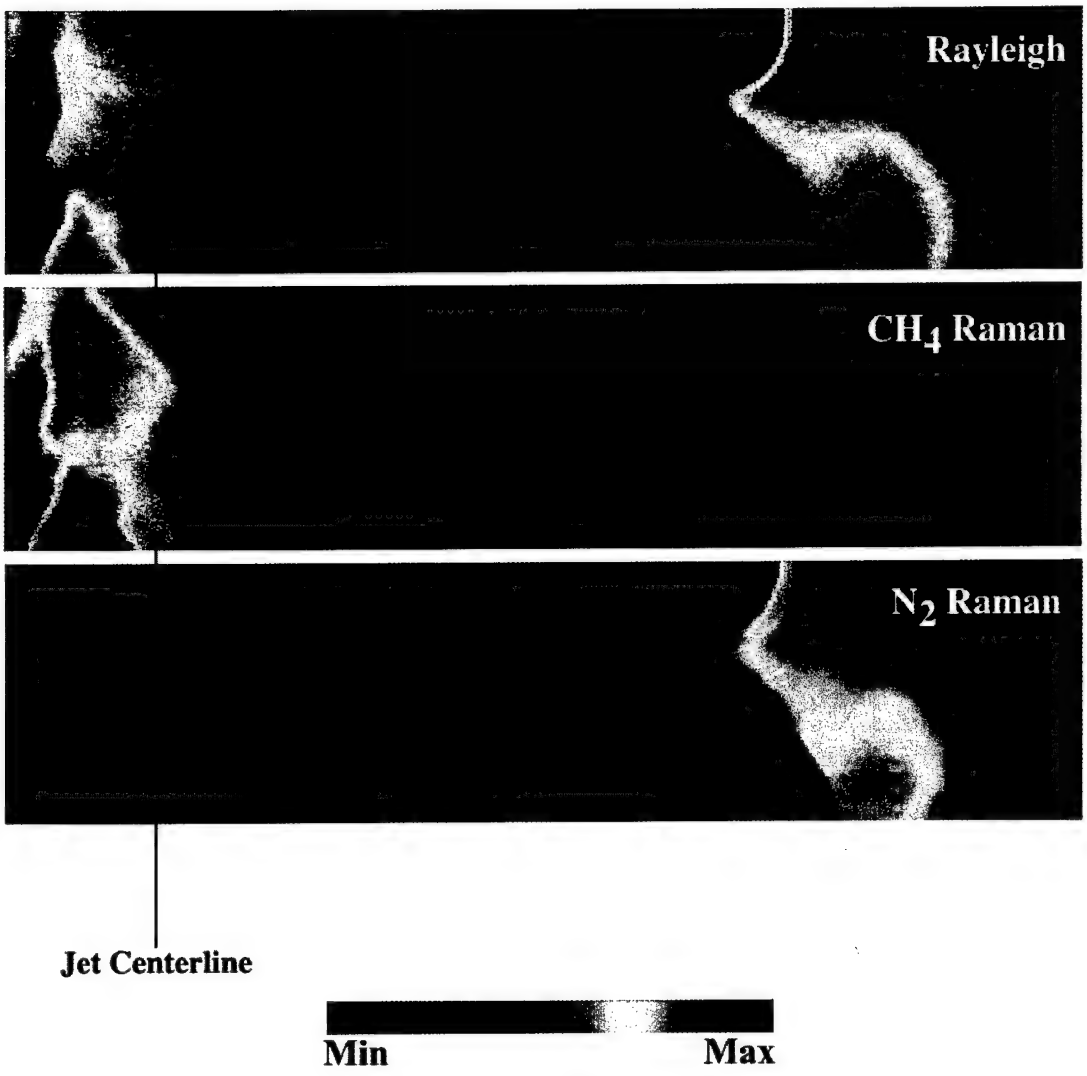

Figure 8. Instantaneous Rayleigh, CH_4 Raman, and N_2 Raman images of the turbulent flame.

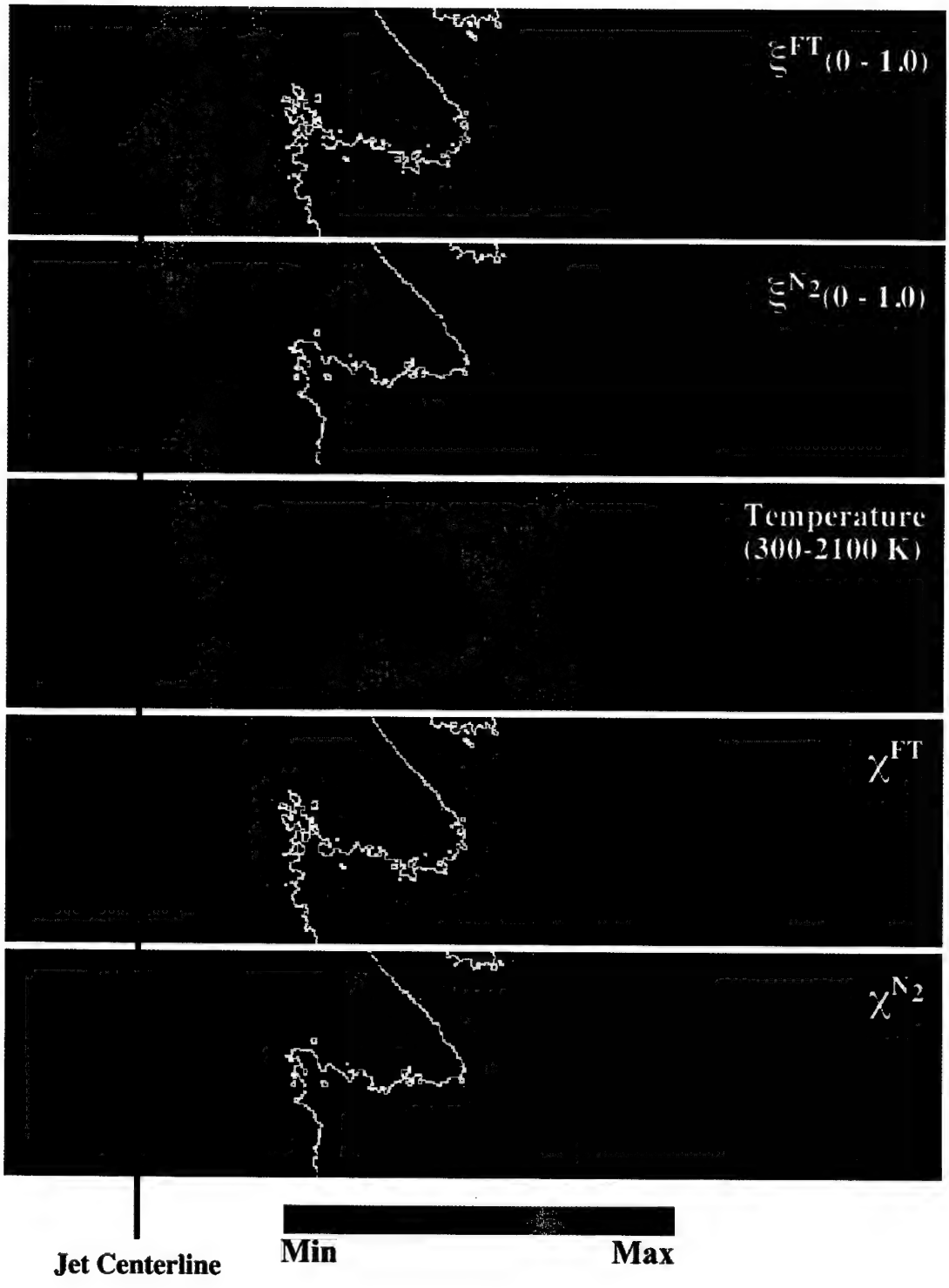

Figure 9. Instantaneous computed mixture fraction images ξ^{FT}, ξ^{N_2}, temperature, and scalar dissipation images χ^{FT}, and χ^{N_2}.

Optical Flow Velocimetry (OFV)

Extending the mixture fraction imaging approach to include simultaneous planar velocity data is extremely desirable. Such measurements would give direct information on scalar fluxes and would be valuable for validating model assumptions. The availability of multi-dimensional velocity and scalar measurements would allow further characterization of the flames by providing information on the relationship of scalars and their gradients with the vorticity and strain rate.

Planar imaging of the velocity field in reacting and non-reacting flows is typically obtained by imaging of Mie-scattering from particles, either with PIV or particle tracking velocimetry (PTV). In a previous funding period, we demonstrated that PIV can be combined with scalar measurements using PLIF [14]. However, particle-based techniques complicate simultaneous laser-based measurements of certain scalar quantities due to interference from the seed particles. In particular, simultaneous imaging of Rayleigh scattering is impossible, making temperature and mixture fraction measurements difficult. A number of "non-particle" velocimetry approaches have been applied in turbulent flows, though few have found broad applicability under reacting conditions [15-17].

Optical flow is concerned with the apparent motion of an image (or brightness) pattern between two frames [18]. Under well-posed conditions, the optical flow will faithfully characterize the actual motion field giving rise to the sequential images. Several optical flow methodologies exist, and the more common approaches are based on either differential techniques or region-based matching [19]. In recent work, we have examined region-based approaches [20] because these do not suffer from the difficulties associated with numerical differentiation or the requirement of small displacements (~1 pixel/frame) as is the case with differential techniques. These and other approaches can at best provide an approximation to the instantaneous two-dimensional fluid velocity given a planar scalar measurement. The approximation is valid when the velocity in the third, unmeasured direction is small, or the scalar gradient in that dimension is small [21].

Although the various approaches are sometimes calibrated using synthetic images [22], direct comparisons between velocities obtained from optical flow and PIV are not available. In an attempt to fill this gap, we performed preliminary experiments in an isothermal turbulent jet of air seeded with both acetone and alumina particles. The experimental configuration is shown in Fig. 10. The nozzle used in these experiments consists of simple tube with a squared-off end (6.35 mm OD; 4.57 mm ID). The turbulent jet issues into an unconfined low velocity coflow of air (~1 m/s). The illumination source consists of the fourth harmonic (266 nm) of an Nd:YAG laser (Continuum, Powerlite 8000) which is formed into a sheet approximately 5 mm high with a beam energy of ~2.5 mJ per pulse. The laser is operated in dual-pulse mode with a pulse separation of 57 μs. The camera employed for the acetone fluorescence is a dual-frame Cooke Corp./PCO SensiCam with an interline progressive-scan CCD (1280 x 1024 pixels). This camera allows the acquisition of two exposures separated by as little as 200 ns. The primary collection lens is a large-format camera objective (Canon, 85 mm, $f/1.2$) with a

corresponding magnification of 31 pixels/mm. A glass filter (Schott, WG305) is used to minimize residual Mie scattering. The acetone fluorescence is broadband, peaking around 430 nm. This setup allows the acquisition of two acetone fluorescence images for use in optical flow velocimetry (OFV). A Photometrics CH350 camera with a UV sensitive CCD coating (QE=10%) and a Nikon Nikkor UV lens (f/4.5) allows direct imaging of the Mie scattering from the seed particles. The two particle scattering frames are spatially separated on the CCD by operating a rotating mirror at approximately 50 Hz.

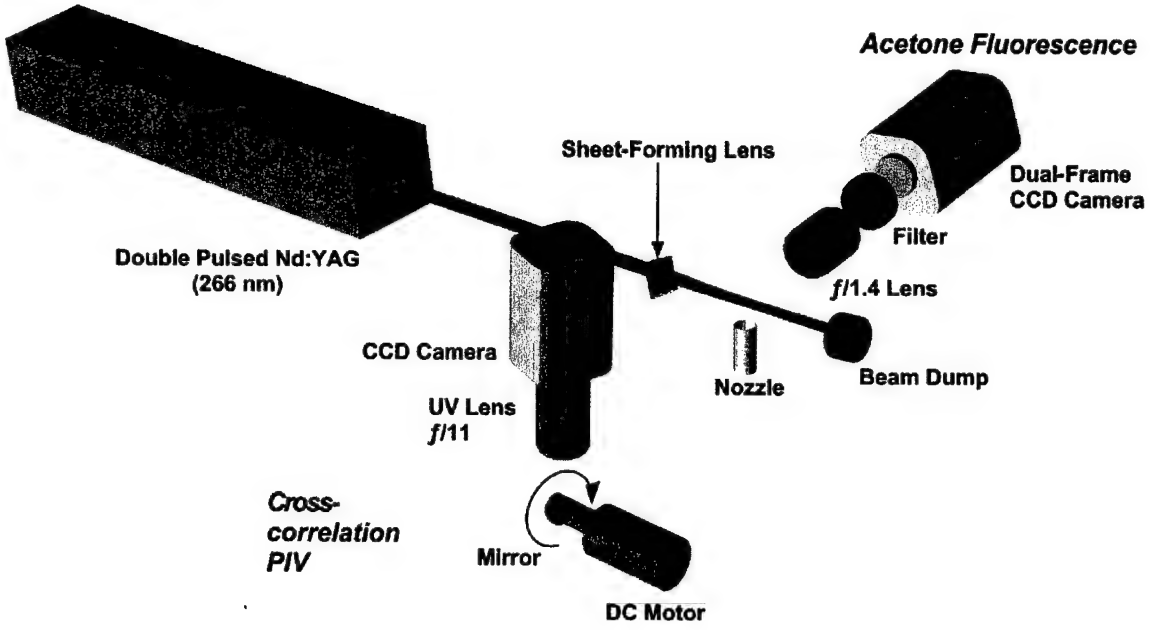

Figure 10. Experimental configuration for the two-camera cross-correlation PIV and acetone fluorescence scalar imaging OF velocimetry validation.

Single-shot scalar images from the turbulent non-reacting flow (Re=2810) are shown in Fig. 11, where the color scale indicates concentration. From this pair of images, the corresponding PIV results and OFV using two different algorithms are shown in Fig. 12. Further details regarding the algorithms will be available in an upcoming paper [23]. Qualitatively, the results are promising, however, further detailed analysis is required to determine the strengths of particular algorithms and lead to a unified OFV approach suitable for a wide range of conditions including reacting flows.

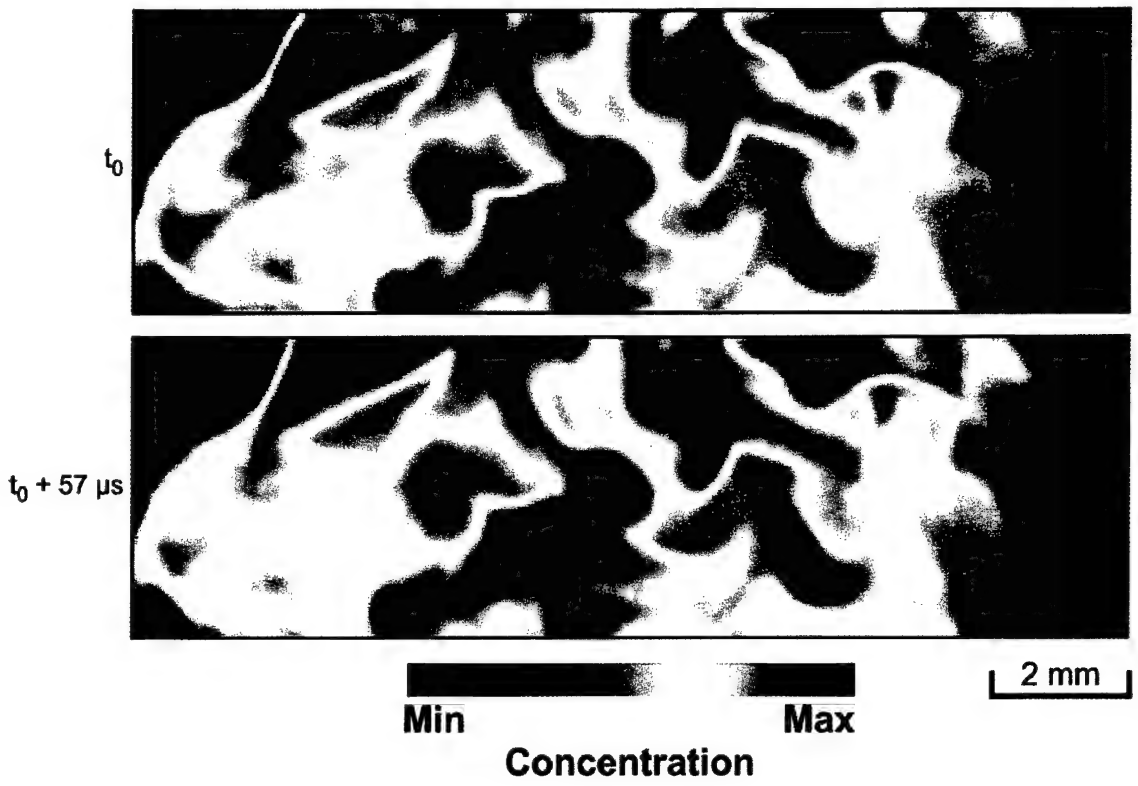

Figure 11. Scalar fluorescence images taken in an turbulent, isothermal jet of acetone-seeded air.

In summary, proof-of-concept experiments were performed within the current funding period to compare simultaneous optical flow velocimetry (OFV) and conventional PIV. In OFV, velocity vectors are computed based upon the displacement fields of molecular flow tracers which would allow concurrent measurement of mixture fraction using the two-scalar approach. Significant progress has been made in implementing exemplar cross-correlation based OFV algorithms, and future work in the areas of diagnostics and computational methodology will result in rapid advances in the field. Current results have been made available to other researchers via the World Wide Web to have broader impact and encourage new development [24].

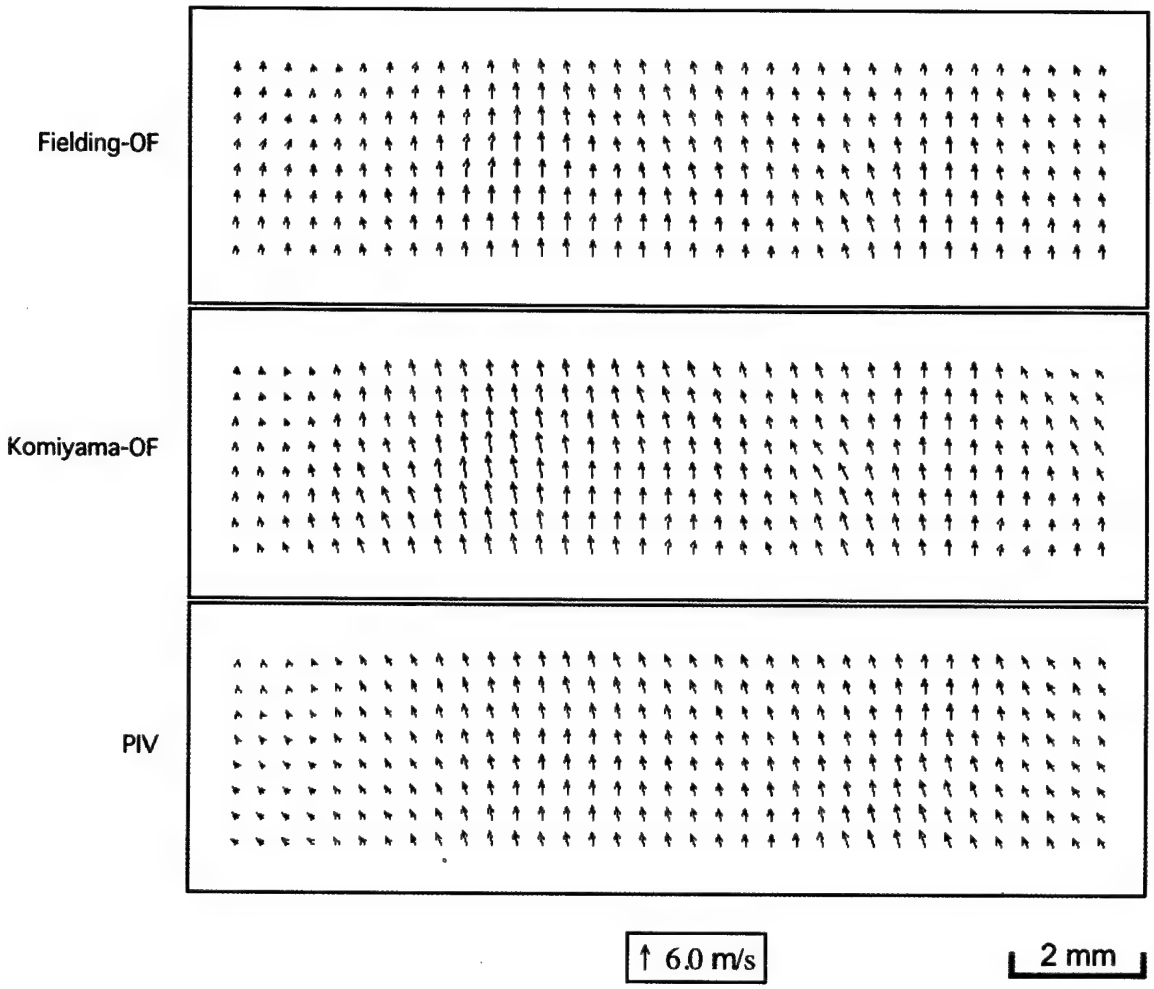

Figure 12. Velocity fields corresponding to the images of Fig. 11. Two different optical flow velocity fields are shown, labeled Komiyama–OF and Fielding–OF to designate the algorithm employed. The third vector field is determined using PIV from simultaneous particle images (not shown).

Additional Research Developments

The dual-frame camera used in the OFV/PIV experiment offers additional capability beyond velocimetry applications (both PIV and optical flow techniques). The fast electronic shuttering (down to 100 ns) offers the possibility of eliminating additional optical components necessary in intensified systems where gateability is the only requirement. This improves the spatial resolution of the imaging system.

To demonstrate this, a turbulent air-diluted methane flame (54% CH_4, 46% air by volume) was examined with the non-intensified imaging system. This blue, moderately sooty flame was selected in order to assess the ability to discriminate against flame interference using the camera's fast shutter capability. For this experiment, a flashlamp-pumped dye laser (Candela, LFDL-20, 1.2 J/pulse) was employed for Rayleigh scattering measurements. The luminosity was integrated single-shot for 4 μs (to bracket the duration of the 2 μs dye laser pulse) and 1000 μs, where the latter value was intended to be representative of a CCD camera operating with a conventional mechanical shutter and minimum 1 ms exposure time. In the fast shutter case, luminosity accounts for less than 5% of the signal relative to a standard helium background image, and about 3% of the signal in the hot zone of the flame. This contrasts with the long exposure case where these values increase to 48% and 25%, respectively.

Subsequent studies of the electronic gating capability were carried out during laser-induced incandescence (LII) experiments in a pure ethylene laminar flame. The LII signal has a duration of several hundred nanoseconds, and an intensifier gate time of ~1 μs is common. In this case, the extremely bright flame luminosity leaks around the mask of the interline CCD frame, increasing the background contribution to the imaged signal and consequently, degrading the dynamic range of the weaker LII signal. Thus, current electronic gating features of fast-frame cameras must be employed with caution according to the particular application. Unintensifed Rayleigh measurements in turbulent nonpremixed flames are possible when using the common air-dilution to minimize soot production. The improvement in spatial resolution will positively impact the scalar dissipation measurements described in this report.

REFERENCES

1. Stårner, S.H., Bilger, R.W., Dibble, R.W., and Barlow, R.S., "Measurements of Conserved Scalars in Turbulent Diffusion Flames," *Combust. Sci. and Tech.* 86:223-236 (1992).
2. Frank, J.H., Lyons, K.M., Marran, D.F., Long, M.B., Stårner, S.H., and Bilger, R.W., "Mixture Fraction Imaging in Turbulent Nonpremixed Hydrocarbon Flames," *Twenty-Fifth Symposium (International) on Combustion*, The Combustion Institute, Pittsburgh, PA, 1994, pp. 1159-1166.
3. Long, M.B., Frank, J.H., Lyons, K.M., Marran, D.F., and Stårner, S.H., "A Technique for Mixture Fraction Imaging in Turbulent Nonpremixed Flames," *Ber. Bunsenges. Phys. Chem.*, 97:1555-1559 (1993).
4. Stårner, S.H., Bilger, R.W., Lyons, K.M., Frank, J.H., and Long, M.B., "Conserved Scalar Measurements in Turbulent Diffusion Flames by a Raman and Rayleigh Ribbon Imaging Method," *Combust. Flame,* 99:347-354 (1994).
5. Stårner, S.H., Bilger, R.W., Frank, J.H., Marran, D.F., and Long, M.B., "Mixture Fraction Imaging in a Lifted Methane Jet Flame," *Combust. Flame*, 107, 307-313 (1996).
6. Stårner, S.H., Bilger, R.W., Long, M.B., Frank, J.H., and Marran, D.F., "Scalar Dissipation Measurements in Turbulent Jet Diffusion Flames of Air Diluted Methane and Hydrogen," *Combust. Sci. Tech.* 129:141-163 (1997).
7. Stårner, S.H., Bilger, R.W., Frank, J.H., Marran, D.F., Long, M.B., "Measurements of Mixture Fraction and Scalar Dissipation in a Turbulent Hydrogen Diffusion Flame," paper presented at the *15th International Colloquium on the Dynamics of Explosions and Reactive Systems*, University of Colorado, Boulder, CO, July 30 - August 4 (1995).
8. Daily, J.W., and Chan, C., "Laser-Induced Fluorescence Measurement of Sodium in Flames," *Combust. Flame.* 33:47-53 (1978).
9. Fielding, J., Schaffer, A.M., Long, M.B., "Three-Scalar Imaging in Turbulent Nonpremixed Flames of Methane," *Twenty-Seventh Symposium (International) on Combustion*, The Combustion Institute, Pittsburgh, PA, 1998, pp. 1007-1014.
10. Bilger, R.W., Stårner, S.H., and Kee, R.J., "On Reduced Mechanisms for Methane-Air Combustion in Nonpremixed Flames," *Comb. and Flame*, 80:135-149 (1990).
11. Namazian, M., Schefer, R.W., and Kelly, J., "Scalar Dissipation Measurements in the Developing Region of a Jet," *Comb. and Flame*, 74:147-160 (1988).
12. Kelman, J.B., and Masri, A.R., *Combust. Sci. and Tech.* 129:17-55 (1997).
13. Stårner, S.H., Bilger, R.W., and Long, M.B., "A Method for Contour-Aligned Smoothing of Joint 2D Scalar Images in Turbulent Flames," *Combust. Sci. and Tech.* 107:195-203 (1995).
14. J.H. Frank, K.M. Lyons, and M.B. Long, "Simultaneous Scalar/Velocity Field Measurements in Turbulent Gas-Phase Flows," *Combust. Flame*, 107:1-12 (1996).
15. Komiyama, M., Miyafuji, A., Takagi, T., "Flamelet Behavior in a Turbulent Diffusion Flame Measured by Rayeligh Scattering Image Velocimetry," *Twenty-Sixth*

Symposium (International) on Combustion, The Combustion Institute, Pittsburgh, PA, pp. 339-346 (1996).
16. Grunefeld, G., Graber, A., Diekmann, A., Kruger, S., Andresen, P., "Measurement System for Simultaneous Species Densities, Temperature, and Velocity Double-pulse Measurements in Turbulent Hydrogen Flames," *Combust. Sci. and Tech.*, **135**:135-152 (1998).
17. Levy, Y., Golovanevsky, B., Kowalewski, T.A., "Fluid Image Velocimetry for Unseeded Flow," *9th International Symposium on Applications of Laser Techniques to Fluid Mechanics*, Lisbon, Portugal, July 13-16 (1998).
18. Horn, B.K.P. and Schunk, B.G., "Determination of Optical Flow," *MIT Artificial Intelligence Laboratory* , Memo No. 572 (1980).
19. Barron, J.L., Fleet, D.J., and Beauchemin, S.S., "Performance of Optical Flow Techniques," *Int. J. Comp. Vision,* 12:43-77 (1994).
20. Anandan, P., "A Computational Framework and an Algorithm for the Measurement of Visual Motion," *Int. J. Comp. Vision,* 2:283-310 (1989).
21. Tokumaru, P.T., Dimotakis, P.E., "Image Correlation Velocimetry," *Exp. In Fluids*, 19:1-15 (1995).
22. Quénot, G.M., Pakleza, J., and Kowalewski, T.A., "Particle Image Velocimetry with Optical Flow," *Exp. In Fluids*, 25:177-189 (1998).
23. Fielding, J., Fielding, G.C., Komiyama, M., and, Long, M.B., "Optical Flow Velocimetry for Turbulent Reacting Flows", manuscript in preparation for special issue of *Applied Optics* (2000).
24. Fielding, J. and Long, M.B., *http://cld3.eng.yale.edu/fielding*

PUBLICATIONS RESULTING FROM THE RESEARCH

Frank, J.H., Lyons, K.M., Marran, D.F., Long, M.B., Stårner, S.H., and Bilger, R.W., "Mixture Fraction Imaging in Turbulent Nonpremixed Hydrocarbon Flames," *Twenty-Fifth Symposium (International) on Combustion*, The Combustion Institute, Pittsburgh, PA, 1994, pp. 1159-1166.

Long, M.B., Frank, J.H., Lyons, K.M., Marran, D.F., and Stårner, S.H., "A Technique for Mixture Fraction Imaging in Turbulent Nonpremixed Flames," *Ber. Bunsenges. Phys. Chem.*, 97:1555-1559 (1993).

Stårner, S.H., Bilger, R.W., Lyons, K.M., Frank, J.H., and Long, M.B., "Conserved Scalar Measurements in Turbulent Diffusion Flames by a Raman and Rayleigh Ribbon Imaging Method," *Combust. Flame,* 99:347-354 (1994).

Stårner, S.H., Bilger, R.W., and Long, M.B., "A Method for Contour-Aligned Smoothing of Joint 2D Scalar Images in Turbulent Flames," *Combust. Sci. and Tech.* 107:195-203 (1995).

Stårner, S.H., Bilger, R.W., Frank, J.H., Marran, D.F., and Long, M.B., "Mixture Fraction Imaging in a Lifted Methane Jet Flame," *Combust. Flame*, 107, 307-313 (1996).

J.H. Frank, K.M. Lyons, and M.B. Long, "Simultaneous Scalar/Velocity Field Measurements in Turbulent Gas-Phase Flows," *Combust. Flame*, 107:1-12 (1996).

Stårner, S.H., Bilger, R.W., Long, M.B., Frank, J.H., and Marran, D.F., "Scalar Dissipation Measurements in Turbulent Jet Diffusion Flames of Air Diluted Methane and Hydrogen," *Combust. Sci. Tech.* 129:141-163 (1997).

Fielding, J., Schaffer, A.M., Long, M.B., "Three-Scalar Imaging in Turbulent Nonpremixed Flames of Methane," *Twenty-Seventh Symposium (International) on Combustion*, The Combustion Institute, Pittsburgh, PA, 1998, pp. 1007-1014.

Fielding, J., Fielding, G.C., Komiyama, M., and, Long, M.B., "Optical Flow Velocimetry for Turbulent Reacting Flows", manuscript in preparation for special issue of *Applied Optics* (2000).

SCIENTIFIC COLLABORATORS

In addition to the Principal Investigator, the following people have participated in this project:

Outside Scientists:	Robert Barlow (*Sandia National Laboratory*) Robert Dibble (*University of California at Berkeley*) Jonathan Frank (*Sandia National Laboratory*) Masaharu Komiyama (*Osaka University*)
Graduate Students:	Joseph Fielding Andrew Schaffer

DEGREES AWARDED

Kevin M. Lyons, Ph.D., May 1994. (Advisor, M. B. Long)

Jonathan Frank, Ph.D., May 1995. (Advisor, M. B. Long)

David Marran, Ph.D., May 1997. (Advisor, M. B. Long)

Joseph Fielding, M.Phil., Dec. 1999. (Advisor, M. B. Long)

LECTURES PRESENTED ABOUT THE RESEARCH

"Mixture Fraction Imaging in Turbulent Nonpremixed Flames," Department of Mechanical Engineering, Yale University, New Haven, CT, September 18, 1996.

"Mixture Fraction Imaging in Turbulent Nonpremixed Flames," Department of Mechanical and Aerospace Engineering, Princeton University, Princeton, NJ, September 24, 1996.

"Quantitative Multiparameter Imaging in Combustion Research," Naval Research Laboratory Chemistry Division Colloquium Series, Washington, D.C. February 20, 1997.

"Quantitative Multiparameter Imaging in Combustion Research," George Washington University, Chemistry Department Seminar Series, Washington, D.C. February 21, 1997.

"Two- and Three-Dimensional Measurements in Flames," ARO/AFOSR Contractors Meeting in Chemical Propulsion, Ohio Aerospace Institute, Cleveland, OH, June 17-19, 1997.

"Multiparameter Imaging in Turbulent Nonpremixed Flames," Poster Presentation at The Gordon Research Conference on Laser Diagnostics in Combustion, Plymouth, New Hampshire, July 6-11, 1997.

"Multiparameter Imaging in Turbulent Nonpremixed Flames," Eastern States Section Meeting of the Combustion Institute, Hartford, Connecticut, August, 1997.

"Quantitative Multiparameter Imaging in Combustion Research," US National Congress on Applied Mechanics, Florida June 21, 1998.

"Two- and Three-Dimensional Measurements in Flames," ARO/AFOSR Contractors Meeting in Chemical Propulsion, Long Beach, CA , June 29, 1998.

"Three-Scalar Measurements for Mixture Fraction Determination in Nonpremixed Methane Flames," International Workshop on Turbulent Nonpremixed Flames, Boulder, CO, July 30, 1998.

"Three-Scalar Measurements for Mixture Fraction Determination in Nonpremixed Methane Flames," International Symposium on Combustion, Boulder, CO, July 30, 1998.

"Quantitative Multiparameter Imaging in Combustion Research," University of Connecticut Department of Mechanical Engineering Seminar Series, Storrs, CT, January 22, 1999.

"Two- and Three-dimensional Measurements in Flames," ARO/AFOSR Contractors Meeting in Chemical Propulsion, Bar Harbor, ME, June 15, 1999.

"Optical Flow Velocimetry for Turbulent Flows and Flames," Eastern States Section Meeting of the Combustion Institute, North Carolina State University, Raleigh, NC, October , 1999.

"Optical Flow Velocimetry for Turbulent Flames," Poster presented at the Gordon Research Conference on Laser Diagnostics in Combustion, Lucca, Italy, June 20-25, 1999.

"Scalar/Velocity Measurements in Turbulent Flows and Flames," Drexel University Department of Mechanical Engineering and Mechanics Seminar Series, Philadelphia, PA, April 21, 2000.

REPORT DOCUMENTATION PAGE

AFRL-SR-BL-TR-00-

0305

1. AGENCY USE ONLY (Leave blank)	2. REPORT DATE	3. REPORT TYPE AND DATES
	5/14/2000	Final Report

4. TITLE AND SUBTITLE

Two- and Three-Dimensional Measurements in Turbulent Flames

5. FUNDING NUMBERS

PE - 61102F
PR - 2308
SA - BS
G - F49620-97-1-0096

6. AUTHOR(S)

Marshall B. Long

7. PERFORMING ORGANIZATION NAME(S) AND ADDRESS(ES)

Department of Mechanical Engineering
Yale University
P.O. Box 208284
New Haven, CT 06520-8284

8. PERFORMING ORGANIZATION REPORT NUMBER

9. SPONSORING / MONITORING AGENCY NAME(S) AND ADDRESS(ES)

AFOSR/NA
801 North Randolph Street
Room 732
Arlington, VA 22203-1977

10. SPONSORING / MONITORING AGENCY REPORT NUMBER

11. SUPPLEMENTARY NOTES

12a. DISTRIBUTION / AVAILABILITY STATEMENT

Approved for public release; distribution is unlimited

12b. DISTRIBUTION CODE

13. ABSTRACT ***(Maximum 200 Words)***

As part of an ongoing research program aimed at developing techniques capable of quantitative imaging of mixture fraction and scalar dissipation in turbulent flames, three-scalar measurements were made in a turbulent nonpremixed flame. The use of nitrogen Raman scattering to detect a passive conserved scalar made it possible to increase confidence in the two-scalar technique based on simultaneous imaging of Rayleigh scattering and fuel Raman scattering. These experiments showed that proper parameterization of mixture fraction-dependent terms appearing in the expression for mixture fraction can improve accuracy for lean values of mixture fraction as well as those near stoichiometric. Additionally, a new experimental technique was investigated which allows the extraction of velocity information from laser-based scalar imaging in turbulent flows. Preliminary results from simultaneous particle-imaging velocimetry (PIV) and optical flow velocimetry showed that this technique has potential for unseeded velocity measurements compatible with the mixture fraction imaging. The optical flow approach was based on extracting velocity vectors from the intensity variations naturally present in inhomogeneous turbulent flow images of a mixing-dependent scalar quantity.

14. SUBJECT TERMS

Turbulent combustion, laser diagnostics, mixture fraction, scalar dissipation, nonpremixed flames, optical flow, velocimetry

15. NUMBER OF PAGES 26

16. PRICE CODE

17. SECURITY CLASSIFICATION OF REPORT	18. SECURITY CLASSIFICATION OF THIS PAGE	19. SECURITY CLASSIFICATION OF ABSTRACT	20. LIMITATION OF ABSTRACT
Unclassified	Unclassified	Unclassified	UL